On the Development of Adaptive, Tendon-Driven, Wearable Exo-Gloves for Grasping Capabilities Enhancement

Lucas Gerez[1], Junan Chen[1], and Minas Liarokapis[1]

***Abstract*—Soft, under-actuated and compliant robotic exo-gloves have received an increased interest over the last decade. Possible applications of these systems range from augmenting the capabilities of healthy individuals to restoring the mobility of people that suffer from paralysis or stroke. Despite the significant progress in the field, most existing solutions are still heavy and expensive, they require an external power source to operate, and they are not wearable. In this paper, we focus on the development of adaptive (underactuated and compliant), tendon-driven, wearable exo-gloves and we propose two compact, affordable and lightweight assistive devices that provide grasping capabilities enhancement to the user. The devices are experimentally tested and their efficiency is validated using three different types of tests: i) grasping tests that involve different everyday objects, ii) force exertion capability tests that assess the fingertip forces that can be exerted while using the exo-gloves, and iii) motion tracking experiments focusing on the finger bending profile. The devices are able to significantly enhance the grasping capabilities of their user with a weight of 335 g and a cost of 92 USD for the body powered version and a weight of 562 g and a cost of 369 USD for the motorized exo-glove version.**

***Index Terms*—Physically Assistive Devices; Prosthetics and Exoskeletons**

I. Introduction

THE human hand is one of the most complex structures of the human body and Nature's most versatile and dexterous end-effector. Roboticists have always been inspired by the human hand, and they constantly seek new ways of transferring the human skills to robotic platforms, enabling them to execute complex everyday life tasks that require increased dexterity (e.g., grasping and manipulating objects or physically interacting with the environment surrounding them) [1]. According to [2], a small set of representative grasp types accounts for more than 80% of the grasp configurations needed during activities of daily living. The grasps used for such activities include the cylindrical, spherical, tridigital, tip (precision grasp), and lateral grasp [3]. All these grasps can be executed with the thumb, index and middle fingers that are the most important ones, while the ring and pinky fingers appear to have a supplementary role [4]. Such outcomes have been used for the development of simplified robotic devices, that offer lightweight and affordable solutions without compromising their overall efficiency [5].

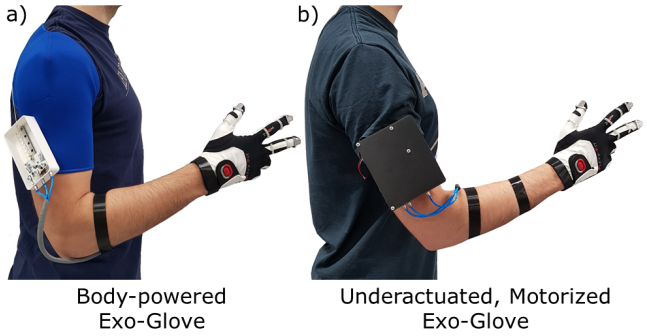

Fig. 1. Side view of the proposed assistive devices (exo-gloves). Both devices are tendon-driven. The body-powered exo-glove of subfigure a) transmits the forces of the upper body (e.g., shoulders) to the human fingers, while the motorized exo-glove of subfigure b) uses a single smart motor (Dynamixel XM430-W350-R) for actuation purposes.

Several studies have focused on the force exertion capabilities of the human hand demonstrating that a healthy individual can generate a maximum grip force that ranges from 300 N to 450 N [6]–[8]. In particular, in [8] the authors conducted experiments to measure the human hand and finger forces in different situations and obtained a mean value of 54 N for pinch grasp forces and 43 N for distal fingerpad forces exerted on flat surfaces. However, most of the activities of daily living, do not require the high contact and grasp forces that humans are capable of exerting. According to [9], the necessary forces to manipulate objects found on activities of daily living do not exceed 10 - 15 N.

The importance of the role of the hand is quite evident in cases of people that suffer from paralysis or stroke. These patients lose some of the capabilities of their hands (e.g., have weaker grasps) and this loss has a tremendous impact on their lives and in some cases on their independence. Over the last decades, the field of exoskeletons, exosuits and in general assistive devices has witnessed an explosive growth. Many wearable, assistive devices have been designed to increase the capabilities of the human hand and to provide assistance to their users to execute activities of daily living (ADLs) or to regain some of the lost dexterity [10], [11]. These wearable devices can be actuated in different ways (e.g., through cables, linkages, hydraulic systems, and inflatable structures) and can have different stiffness, from completely soft to totally rigid.

Manuscript received: September, 10, 2018; Revised November, 28, 2018; Accepted December, 17, 2018. This paper was recommended for publication by Editor Pietro Valdastri upon evaluation of the Associate Editor and Reviewers' comments.

[1]Lucas Gerez, Junan Chen, and Minas Liarokapis are with the New Dexterity research group, Department of Mechanical Engineering, The University of Auckland, New Zealand. E-mails: lger871@aucklanduni.ac.nz, jche932@aucklanduni.ac.nz, minas.liarokapis@auckland.ac.nz

Digital Object Identifier (DOI): see top of this page.

In [12], the authors propose a rigid hand exoskeleton that weighs 1.1 kg and can exert a continuous force of 5 N through linkages and motors connected to the hand. In [5], a tendon-driven soft robotic exo-glove is proposed, that can generate a pinch force of 20 N and a wrap grasp force of 40 N using a battery powered actuation unit that weighs more than 1.5 kg. In [13], the authors present a tendon-driven robotic glove that can apply a maximum grip force of 15 N using a backpack weighing approximately 6 kg. In [14], the authors propose the SEM Glove, a tendon-based assistive glove that can exert up to 4 N in the fingertips using a battery which lasts approximately one day and costs more than 4,000 USD. In [15], the authors present the SSRG glove, a robotic glove used in space suits that employs linear actuators that pull synthetic tendons to increase the grip strength by more than 60 N. In [16], the authors propose an exo-glove that achieves an increase of about 8 N of the distal tip force using a belt pack with a battery and a hydraulic system that weighs 3.3 kg and can run for two hours. In [17], a soft robotic glove is proposed using a pneumatic system to actuate it. This systems weighs 1.26 kg and can exert a maximum fingertip force of 9.12 N.

Although the aforementioned assistive devices can offer a substantial improvement in the quality of life of people with physical disabilities, they have several limitations. First, these devices rely on external power sources to operate, and as a consequence, their autonomy is limited. In addition, the cost of assistive devices increases considerably when pneumatic systems, multiple motors, and sophisticated sensors are used. The addition of these components also increases the total weight of the device, making it also uncomfortable for the user. Last but not least, most of the current wearable solutions do not offer a long operation time so they cannot be used for long periods of time. Thus, a lightweight, affordable, easy to operate assistive device with long autonomy would be indispensable for people that suffer from paralysis or for human augmentation purposes.

In this paper, we propose two compact, wearable, and lightweight assistive exo-gloves for grasping capabilities enhancement. The first device uses a body-powered mechanism while the second device is an underactuated, motorized solution (Fig. 1). The devices are experimentally tested and their efficiency is validated using three different types of tests: i) grasping tests that involve different everyday objects, ii) force exertion capability tests that assess the fingertip forces that can be exerted while using the exo-gloves, and iii) motion tracking analysis of the bending profile of the index finger.

The rest of the paper is organized as follows: Section II presents the designs and the modelling of the devices, Section III details the experimental setup used for the tests and presents the experimental results, while Section IV concludes the paper and discusses future directions.

II. Designs and Modelling

In this section, we present the designs and the modelling of the body-powered and the motorized exo-gloves, discussing also their functionalities and their operation.

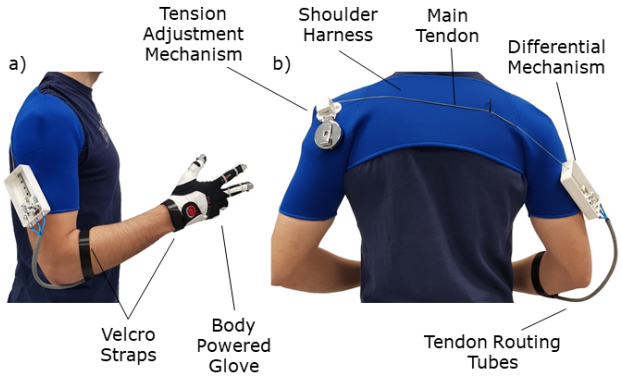

Fig. 2. Annotated presentation of the body-powered device in side view (subfigure a) and back view (subfigure b). The device consists of a harness, a glove, a differential mechanism, a tendon tensioning and adjustment mechanism, tendon routing tubes and artificial tendons. The body-powered mechanism relies on the transmission of forces from the upper body (e.g., shoulders) to the fingers through the tendon routing system. Simple body movements can increase the tension of the tendon, actuating the soft exo-glove. The differential mechanism is used to evenly distribute the forces to the participating fingers.

A. Body-powered Assistive Exo-glove

The body-powered exo-glove was designed to enhance the grasping capabilities of the user, providing easiness and intuitiveness of operation, with long autonomy, low maintenance, and low cost. The device consists of four different parts: the differential module, the soft glove, the tendon tensioning and adjustment mechanism, and the harness (see Fig. 2).

The differential module is a solution for tendon tensioning and even distribution of the grasping forces for the participating fingers. The particular differential mechanism can also be applied to different underactuated prosthetic and orthotic systems. Differentials based on the whiffletree mechanism are widely used in underactuated robot hands [18], [19]. Fig. 3 shows an annotated image of the proposed solution. The differential is divided into three different parts: the ratchet clutch, the linear ratchet, and the spring loaded whiffletree mechanism. The ratchet clutch mechanism consists of a ratchet-pulley block for tendon wrapping, a pawl that blocks the rotation of the ratchet in one direction and an elastic element that acts as a spring and pushes the pawl against the ratchet teeth, constraining its motion in the other direction. This mechanism allows a fine and precise adjustment of the tendon length (with a precision of 0.87 mm) [20]. The purpose of using this mechanism is to adjust the length of multiple tendons that are routed through the tendon routing tubes and reach the glove. In order to keep the tendon tensioned for a long time, a linear ratchet was used. This mechanism guarantees that the tendon is locked in one position until the mechanism is used again. This mechanism consists of several "V" shape teeth arranged on a row, a lever, a rail, a base, and two springs. The rail is fixed to the differential module through screws and the base can slide on the rail guaranteeing that the motion of the base always happens on a single axis. When the upper cable is pulled, the lever is pushed by a spring against the teeth until the system reaches the desired position. Then, the lever slides into one of the "V" shape teeth locking

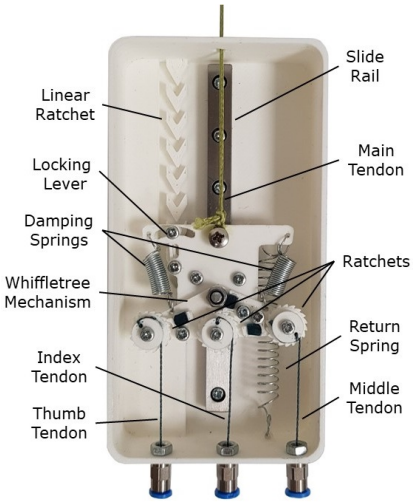

Fig. 3. The proposed spring loaded differential mechanism is a solution for tendon termination, tensioning and locking that can be applied not only to assistive exo-gloves but also to robot and prosthetic hands. The concept is based on an even distribution of the body-powered mechanism forces to the participating finger tendons using the whiffletree mechanism. The differential can be efficiently locked in different positions using a linear ratchet and a locking lever. When the main tendon is pulled, the locking lever is pushed by a spring against the teeth of the linear ratchet until the system is locked at the desired position. The finger tendons are terminated on the whiffletree differential mechanism using the ratchet clutch system proposed in [20].

the mechanism and keeping the tension constant. When the system is re-engaged, the lever is pulled again to the channel and a spring that connects the base to the differential module walls pulls the base until the lever reaches its lowest position and the tendon returns to its initial tension. When the upper cable is pulled again the cycle is reinitialized. The ability to keep the tendons tensioned for long periods of time is of paramount importance for underactuated and body-powered systems, since in other tendon-driven, motorized solutions (e.g., fully-actuated systems) the dedicated motors can adjust the tensioning of the tendons and hold the load while the grasping and manipulation of the objects take place.

The body-powered mechanism allows the transmission of forces from the upper body (e.g., the shoulders) to the index, middle, and thumb fingers through the tendon routing system. Simple body movements can increase the tension of the tendon, actuating the soft exo-glove. The differential mechanism is used to evenly distribute the forces to the fingers. In order to operate the device, this cable must be accurately tensioned and for this purpose, a tension adjustment mechanism was designed. The mechanism consists of a base where the parts are connected, a lever, a pulley with rectangular teeth, a cover and a retractable reel. After wearing the mechanism, the user presses a lever and the cable on the reel (separate from the tendon) rotates the pulley in the counterclockwise direction wrapping the actuation tendon around it and tensioning it. The plastic cover guarantees that the cable does not slip out of the pulley channel.

The proposed harness was chosen for the body-powered device because it is comfortable and helps to keep the shoulders aligned. When the right arm or the shoulders move transmitting forces to the main cable, the differential is pulled and the artificial tendons of the fingers are tensioned. These tendons are in charge of moving the fingers and they are made out of a low friction braided fiber of high-performance UHMWPE (Ultra-High Molecular Weight Polyethylene). One end of the tendon is terminated on the differential mechanism and the other end on a stainless steel structure at each fingertip. It must be noted that the execution of tasks with the body-powered mechanism takes longer due to the longer body compensation motions that are required to actuate the exo-glove. The body-powered exo-glove was designed to be as simple and straightforward as possible to allow people to use it without intense training. The device can be adjusted to all body types and sizes. The personalization occurs only for the glove and the harness because the size of these items depends on the user's height and weight.

The prototype of the body powered mechanism costs 92 USD to produce and weighs 335 g. To the best of our knowledge this is the lightest among all the assistive exo-gloves currently found in the literature. It is important to highlight that this solution can be extended to different actuation units. The force transmission from the shoulder to the fingertips could be executed by other members or external systems if the person cannot use other body parts (e.g., a motor could replace the tension adjustment mechanism to tension the cable that comes from the spring loaded differential mechanism).

B. Underactuated Motorized Assistive Exo-glove

The motorized assistive exo-glove was designed to enhance the grasping capabilities, providing the user easiness of operation and high grasp forces with minimum effort. The device is divided into three different parts: a control box, an EMG (Electromyography) sensor, and the soft glove (Fig. 4).

The operation of the device is straightforward and as simple as the body-powered device. An EMG sensor is connected to the user's forearm in a region where high variation in the electrical activity of the muscles can be sensed (*Flexor Digitorum Superficialis* area). The EMG sensor board detects muscle activities that are related to grasping, filters, rectifies, and computes the envelope of the signals by integrating them, and sends them to the microcontroller, where they are processed. The microcontroller, the sensor, and the motor are powered by a 2200mAh 3S 20C Li-Po battery (see Fig. 5). The microcontroller controls the motor via simple thresholding of EMG signals, to actuate the exo-glove. The motor is connected to a differential mechanism with two pulleys. These pulleys are connected to the tendons that reach the fingertips of the glove and they are in charge of actuating the fingers (one pulley drives the tendon connected to the thumb and the other drives the tendons connected to the index and middle fingers). While the transmission of motion is instantaneous for the body-powered device, the motorized device presents some delay between the EMG sensor reading and the motor actuation, a delay that increases slightly the task execution time.

The differential mechanism operates similarly to the popular differentials found in cars (but using spur gears), distributing the power of the motor to two shafts. The differential mechanism allows not only torque distribution but also the pulleys

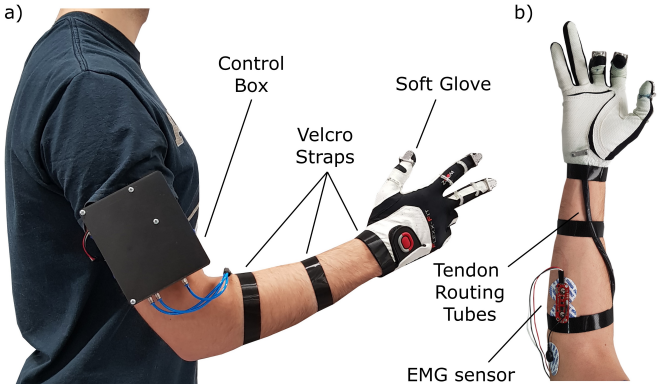

Fig. 4. Annotated presentation of the motorized assistive device in side view (subfigure a) and forearm view (subfigure b). The device consists of a control box, an EMG sensor, and a glove. The operation of the device is based on a simple surface Electromyography (EMG) interface. An EMG sensor is used to measure the activity of the muscles of the forearm (e.g., flexor digitorum superficialis) and the EMG signals are processed, rectified, filtered and used to control (via simple thresholding) a smart motor that actuates the tendon-driven, exo-glove.

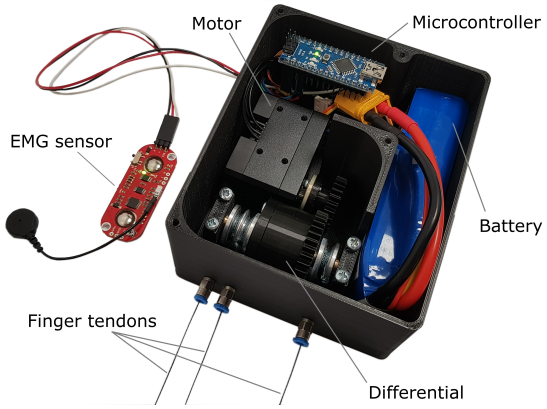

Fig. 5. The control box consists of a smart motor (Dynamixel XM430-W350-R), a battery (Li-Po 2200mAh 3S 30C), a microcontroller (Arduino Nano), and a differential mechanism. The EMG sensor (MyoWare muscle sensor) is attached on the forearm skin, and is used to detect the muscle activities that will lead to a grasping motion. The EMG signals are processed, rectified, filtered, and used to control the motor, actuating the soft exo-glove via simple thresholding. The motor is connected to a differential mechanism that distributes the power of the motor to two shafts that are connected to finger-specific pulleys. The differential mechanism allows for an even torque distribution but also the pulleys to rotate in different speeds when the force distribution is uneven.

to rotate in different speeds when the force distribution is uneven. This helps the user during grasping, distributing the forces between the fingers and providing a more stable grasp. Moreover, the use of a differential mechanism reduces the need for an extra motor, reducing also the cost and the weight of the final device.

The prototype weighs 562 g and costs 349 USD to produce, more than ten times less than the commercial version of another assistive device found in [14]. Autonomy tests have been conducted and the prototype can operate for more than 6,000 grasp cycles with the same battery. The proposed system weighs less than half of most of the devices analyzed in [5], [13], [16], [17] and has an operation time of an entire day, based on the number of grasps that humans typically execute in 24 h [21].

C. Soft Exo-glove

The soft glove system used on the device is composed of a thin, tight-fit, high sensibility glove (golf glove), three anchor structures (for thumb, index and middle fingers), five soft anchor points, three artificial tendons and one cable support. The system was designed so as to maximize the tactile sensitivity, dexterity and grasping forces that the user can exert during the execution of tasks. In order to increase the friction between the object and the exo-glove, a glove with a rubbery cover was selected. A unique design attribute of this solution is the use of internal tendons in the glove. External cables can be obstructed while grasping by the objects, damaging the cable or decreasing the efficiency of the device. At the fingertip, a stainless steel anchor structure was stitched at the back of the glove, as shown in Fig. 6. The design decision to actuate only three fingers (index, middle, and thumb) was based on their importance in executing most tasks of daily living [21]. The final design of the exo-glove, including all components attached to it, weighs no more than 55 g, less than half of the weight of the gloves found in [10].

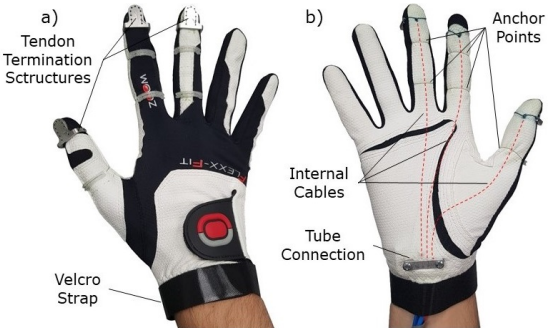

Fig. 6. Annotated view of the soft exo-glove used by both devices. It consists of a thin, tight-fit, high sensitivity glove, three internal tendons, a tube connection, three stainless steel termination structures (at the fingertips) and five anchor points for tendon rerouting. The tubes connect the differential mechanism to the exo-glove and they are fixed at the exo-glove side by a tube connection made out of aluminum. The force transmission is done by artificial tendons that are terminated on the whiffletree at the differential side and on the termination structures at the exo-glove side. All the tendons are routed inside the glove. The soft anchor points offer better sensibility of the grasped objects than the rigid anchor points, making also the design more lightweight, more compact and aesthetically pleasing.

Three 3 mm polyurethane tubes are used for tendon routing. They are attached to the exo-glove through two aluminum structures that are screwed against each other on the exo-glove. A Velcro strap on the wrist is used to hold the tubes and to prevent the deformation of the fabric structure of the exo-glove when the tendon is pulled (a problem previously described in other studies [22]). The main difference between the exo-glove used on this device and the tendon driven assistive exo-gloves found in the literature [5], [13], [23], is the application of soft anchor points at the front of the hand to hold the tendons. Rigid anchor points, reduce sensibility and the contact area between the hand and the object while thin soft anchor points made of braided fiber offer better sensibility of the grasped objects and make the design more lightweight, more

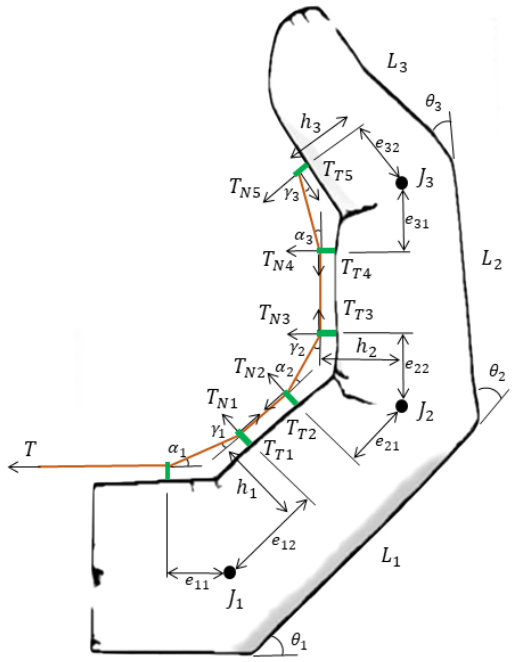

Fig. 7. Model of the tendon routing of a generic finger. L_1, L_2 and L_3 represent the proximal, middle and distal phalanges, while the black circles, J_1, J_2 and J_3, represent the finger joints. The brown line represents the artificial tendon used and the green rectangles represent the anchors points.

compact and aesthetically pleasing. Fig. 6 shows the anchors positions. At the back of the hand, a semicircular 3D printed structure was added and stitched to the exo-glove to prevent the braided fiber from hurting the hand due to the high forces exerted by the artificial tendons. The soft anchor positions were defined using a model of the applicable forces on the anchors generated by the tendons. Fig. 7 illustrates the model. J_1, J_2 and J_3 are the finger joints. The distances L_1, L_2 and L_3 are the lengths of proximal, middle and distal phalanges, respectively, e is the distance between the closest finger joint and the anchor along the sagittal plane, h is the normal distance between the anchor point and the sagittal plane, θ is the angle between two phalanges (the angles applied to this model for each joint can be found at [24]), α and γ are two angles of the triangle created by the tendon and the tangential plane. When an anchor point is added to the exo-glove, if the tendon is tensioned with a force T, it exerts a force to the anchor perpendicularly to the finger, T_N, and tangential to the finger, T_T. The anchor positions should be optimized in such a way that the configuration generates the maximum torque in all three joints (Eq. 1). For this reason, the sum of the torques τ_1, τ_2 and τ_3 should be maximum.

The torques τ_1, τ_2 and τ_3 are given by Eq. 2, 3 and 4, respectively. Each torque is originated by the forces acting at the anchors.

$$\sum_{n=1}^{3} \tau_n = \tau_1 + \tau_2 + \tau_3 \tag{1}$$

$$\tau_1 = T_{N1}e_{12} + T_{N2}(L_1 - e_{21}) + T_{T2}h_1 - T_{T1}h_1 \tag{2}$$

$$\tau_2 = T_{N3}e_{22} + T_{N4}(L_2 - e_{31}) + T_{T4}h_2 - T_{T3}h_2 \tag{3}$$

$$\tau_3 = T_{N5}e_{32} + T_{T5}h_3 \tag{4}$$

The tangential and perpendicular forces can be written in terms of the angles α, γ, and tension T (Eq. 5, 6 and 7).

$$\tau_1 = T[\sin(\gamma_1)e_{12} + \sin(\alpha_2)(L_1 - e_{21}) + \cos(\gamma_1)h_1 - \cos(\alpha_2)h_1] \tag{5}$$

$$\tau_2 = T[\sin(\gamma_2)e_{22} + T\sin(\alpha_3)(L_2 - e_{31}) + \cos(\gamma_2)h_2 - \cos(\alpha_3)h_2] \tag{6}$$

$$\tau_3 = T[\sin(\gamma_3)e_{32} + \cos(\gamma_3)h_3] \tag{7}$$

Using the sines and cosines laws the angles α and γ can be written in terms of angle θ, as shown in Eq. 8 and 9.

$$\alpha_n = \arcsin \frac{e_{n1}\sin(180 - \theta_n)}{\sqrt{e_{n2}^2 + e_{n1}^2 - 2e_{n2}e_{n1}\cos(180 - \theta_n)}} \tag{8}$$

$$\gamma_n = \arcsin \frac{e_{n2}\sin(180 - \theta_n)}{\sqrt{e_{n2}^2 + e_{n1}^2 - 2e_{n2}e_{n1}\cos(180 - \theta_n)}} \tag{9}$$

Replacing the angle values of Eq. 8 and 9 into Eq. 5 to 7, it is possible to verify that the maximum value of torque is obtained when e_{12}, e_{22}, and e_{32} are maximum and, e_{21} and e_{31} are minimum. Based on this model, to maximize the total torque of the finger, the anchors were positioned as shown in Fig. 6. As e_{12} should be maximum and e_{21} minimum, one anchor was added closest to J_2. The same case occurs with e_{22} and e_{31} and for this reason, another single anchor was added closest to J_3. Also, the distance h that is relative to the finger thickness is directly proportional to the torque, meaning that the tendon should be placed as far as possible from the sagittal plane.

III. Experiments and Results

The experiments conducted to assess the performance of the body-powered and the motorized devices were divided into three parts. The first part focused on evaluating the grasping performance for everyday objects, while wearing the exo-gloves. The second experiment focused on measuring the grasping forces (in different configurations) that the devices can exert using a 3D printed model hand inside the glove, as well as measuring the fingertip forces exerted by the exo-glove using the proposed tendon routing model. The third part focused on the analysis of the bending profile of the index finger wearing the assistive devices. Table I and II summarize the results of the first two tests for the body-powered device and the motorized device, respectively.

Fig. 8. Both devices were tested for grasping different types of objects: a) a ball, b) a mustard bottle, c) a jar, d) a glass bottle, e) a spray bottle, and f) tweezers.

TABLE I
SUMMARY OF MAXIMUM EXERTED FORCES AND CHARACTERISTICS OF THE PROPOSED BODY-POWERED DEVICE. THE DESCRIPTION OF THE GRASP TYPES USED CAN BE FOUND IN [8], [25], AND [26].

Description	Value
Pinch grasp force (human hand)	8.2 N
Power grasp force (human hand)	11.6 N
Pinch grasp force (model hand)	8.9 N
Power grasp force (model hand)	13.9 N
Device weight	280 g
Glove weight	55 g
Total weight (including glove)	335 g
Cost	92 USD
Autonomy	∞

TABLE II
SUMMARY OF MAXIMUM EXERTED FORCES AND CHARACTERISTICS OF THE PROPOSED MOTORIZED DEVICE.

Description	Value
Pinch grasp force (human hand)	8.9 N
Power grasp force (human hand)	14.3 N
Pinch grasp force (model hand)	9.1 N
Power grasp force (model hand)	16.4 N
Control box weight	507 g
Glove weight	55 g
Total weight (including glove)	562 g
Cost	369 USD
Autonomy	$>$ 6000 cycles

A. Device-aided Object Grasping - Human Hand

The first test focused on wearing the devices (as shown in Fig. 2 and Fig. 4) to evaluate the grasping performance for different everyday objects. The goal of these tests was to verify if the subject was capable of executing different grasping tasks and handle the objects as a healthy individual. Fig. 8 shows some objects that can be grasped using the proposed devices. When the devices are locked in a position of grasping, it is possible to grasp and retain the object without difficulties due to the constant force applied by the differential in the body-powered device and the motor in the motorized version. In order to evaluate the amount of force exerted by the devices, two different grasping types were used: the pinch grasp and the power grasp. A Biopac MP36 data acquisition unit (Biopac Systems, Inc., Goleta, California) was used with the SS25LA dynamometer to measure the forces exerted in each scenario. For the body-powered device, the maximum force obtained for the pinch grasp and power grasp configurations were 8.2 N and 11.6 N, respectively. For the motorized device, the maximum force obtained for the pinch grasp and power grasp configurations were 8.9 N and 14.3 N, respectively. These pinch and power grasp forces are enough to execute most of the ADLs as discussed in [9], [27] and these forces are within the same force range of devices found in [10]. Although the user was instructed to not exert any forces with his/her fingers during the tests in order to not affect the results, it is necessary to guarantee that no involuntary forces were exerted. For this reason, the experiments were repeated using a model hand.

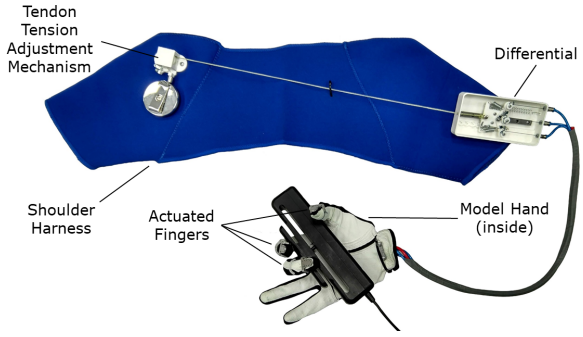

Fig. 9. When the exo-glove is tested by able bodied people the total force exerted may be affected by involuntary human finger motions. In order to run experiments without the human "in-the-loop", we decided to create a model, 3D printed, articulated hand that doesn't have any actuation mechanism (a mannequin hand) and to fit the glove on that hand. The particular hand makes sure that during the standalone exo-glove actuation the soft structure of the glove will bend properly, measuring the exerted contact forces. The figure shows the exo-glove (equipped with the model hand) grasping a dynamometer for force measuring purposes. The maximum force obtained for the power grasp posture was 13.9 N.

B. Device-aided Object Grasping - Model Hand

The second experiment focused on replacing the human hand with a model hand [28] and execute different grasping tasks. This replacement guarantees that during the standalone exo-glove actuation the soft structure of the glove will bend properly (due to the model hand), measuring the required contact forces. Fig. 9 shows the exo-glove grasping a dynamometer for force measuring purposes. The grasp experiments were performed with the body-powered device, obtaining a maximum force of 13.9 N for full grasp and 8.9 N for pinch grasp force. Regarding the motorized device, the values were 16.4 N for power grasp and 9.1 N for pinch grasp. Another experiment was executed, verifying the maximum force that the index and middle fingers could withstand in the hook grip position. The load was incrementally added and the maximum obtained value was 108 N. If compared to the first part of the experiments, it is possible to observe that the order of magnitude of the forces are similar, indicating that tests with subjects wearing the devices are reliable. Slightly higher values of forces were expected for these experiments because the model hand does not have any stiffness in the finger joints, and for this reason, there are no forces acting against the force application direction.

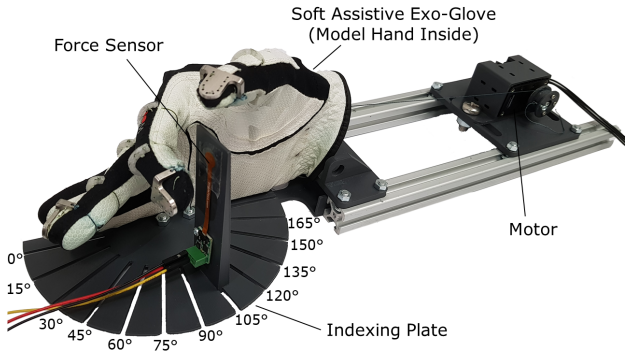

Fig. 10. Experimental setup used for force exertion experiments conducted with an exo-glove fingertip. The setup consists of a model hand (mannequin hand) wearing the proposed soft, assistive, exo-glove, a miniature force sensor (SingleTact S8-100N), an indexing plate with a increment value of 15° and a smart motor (Dynamixel XM430-W350-R) for driving the tendon. The force profiles were acquired for a total of 12 equally spaced angles. The maximum force exerted at each angular position was captured.

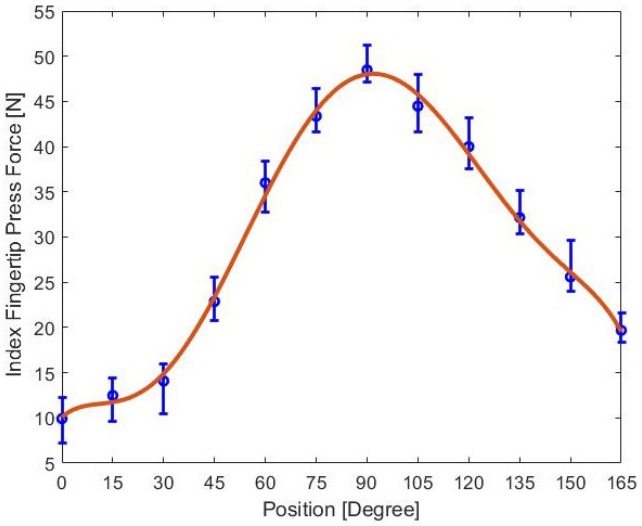

Fig. 11. Results of the exo-glove fingertip force exertion experiments. Data was acquired for 5 experimental trials at each angular position (a total of 12 positions). The red curve was fitted to the mean values of the five trials for all angular positions. The error bar presents the maximum and minimum value of each test. The maximum force exerted was 48 N at 90°.

C. Fingertip Force Exertion Experiment

The particular experiment was executed to assess the fingertip forces exertion capabilities of the exo-glove. The fingertip forces were acquired for 12 equally spaced angles as shown in the setup in Fig. 10. A model hand wearing the soft assistive exo-glove was used to conduct the experiments. During the flexion of the index finger, the force exerted by the fingertip can be measured at different positions, due to the continuous change of the normal direction of the finger distal pad. The maximum force exerted at each angular position was obtained before the fingertip slipped away from the force sensor, due to the finger reconfiguration. Fig. 11 presents the results of this experiment. The force exerted was 10 N at 0° and reached a maximum value of 48 N at 90°. The force values of the remaining sensor positions declined and stopped at 20 N.

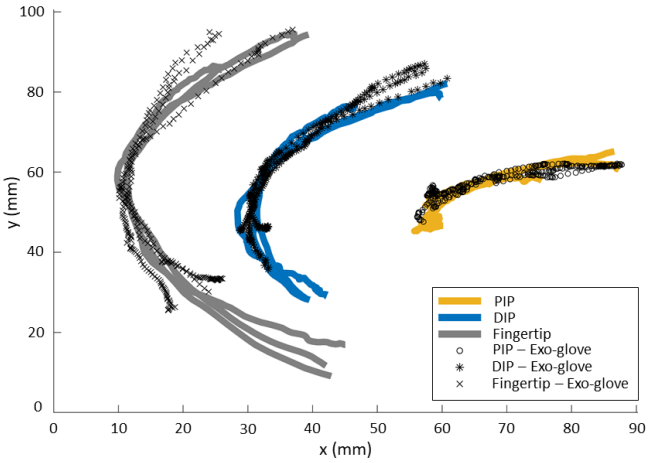

Fig. 12. Results of the motion tracking experiments. The figure shows the bending profile of three finger positions (PIP joint, DIP joint and fingertip) for two conditions: free-hand motion and human hand assisted by the exo-glove. The data demonstrates that the assistive glove provides a similar bending profile for the PIP and DIP joints. For the fingertip, the bending profile also follows the path of the free motion of the human finger, although the range of motion is more restricted.

D. Motion tracking and analysis

The motion tracking and analysis experiment was executed to compare the bending profile of the human finger in free motion with the bending profile of the human finger when it is assisted by the exo-glove.

The experiment was conducted using an optical motion capture system with eight cameras (Vicon Motion System Ltd., UK) to capture the range of motion of one finger in both scenarios. Five reflective markers were attached at the back of the glove to track the bending profile of the index finger, and the experiment was repeated ten times. Fig. 12 shows the paths of the PIP and DIP joints, and the fingertip for the two different scenarios. The bending profile of the finger is affected by the glove design, so the body-powered and the motorized devices display similar ranges of motion. As it can be noticed, the paths of the PIP and DIP joints are similar in both scenarios, but the fingertip paths are significantly different. This difference occurs when the finger motion is assisted by the exo-glove, as the motion of the distal phalanx is restricted up to a specific angle due to the glove design.

E. Video

A video of the devices can be found at the following URL:

http://newdexterity.org/exogloves/

IV. Conclusions and Future Directions

In this paper, we presented a body-powered, assistive exo-glove and an underactuated, motorized, assistive exo-glove to augment the grasping capabilities of healthy individuals and to assist patients with physical disabilities (people that suffer from paralysis or stroke). Experiments were performed to evaluate the performance of the proposed devices, and the results demonstrate that the developed assistive exo-gloves can efficiently enhance the grasping capabilities of their users,

offering lightweight, affordable, and easy to operate solutions that can assist the execution of ADLs. It must be noted that since the body-powered device does not require any external power supply or external actuators and since most of the parts are made out of plastic and can be 3D printed, this makes the device uniquely affordable, easy to operate and easy to replicate. Such a device could provide a good solution for people that live in regions that suffer from poverty or wars. The underactuated, motorized, assistive glove, is also easy to operate providing the user full control of the device, and it may be more useful than the body-powered device for people that a have high level of mobility restriction.

Although the proposed devices have multiple advantages in terms of weight, cost, autonomy, and force exertion capabilities, they also have several limitations. For the body-powered device, the user has to be able to execute body compensation motions that transmit the forces from the upper body to the hand. Patients who suffer from severe paralysis might not be able to execute these motions. For the motorized device, the differential mechanism does not allow us to control independently the forces exerted by the index and middle fingers. Finally, the control box of the motorized device is quite bulky due to the battery dimensions and extra effort should be put into optimizing its volume.

Regarding future directions, we plan to design a mechanism that allows controlling the thumb motion for both devices, not only in closing and opening but also in opposition, in order to increase the dexterity of the devices. For the motorized, assistive exo-glove, we plan to reduce the size of the control box and control the forces applied by each finger to different types of objects according to the data collected from muscle and embedded force sensors.

REFERENCES

[1] C. C. Kemp, A. Edsinger, and E. Torres-Jara, "Challenges for robot manipulation in human environments [grand challenges of robotics]," *IEEE Robotics & Automation Magazine*, vol. 14, no. 1, pp. 20–29, 2007.

[2] C. Sollerman and A. Ejeskär, "Sollerman hand function test: a standardised method and its use in tetraplegic patients," *Scandinavian Journal of Plastic and Reconstructive Surgery and Hand Surgery*, vol. 29, no. 2, pp. 167–176, 1995.

[3] M. C. Carrozza, G. Cappiello, S. Micera, B. B. Edin, L. Beccai, and C. Cipriani, "Design of a cybernetic hand for perception and action," *Biological cybernetics*, vol. 95, no. 6, p. 629, 2006.

[4] M. V. Liarokapis, P. K. Artemiadis, and K. J. Kyriakopoulos, "Quantifying anthropomorphism of robot hands," in *IEEE International Conference on Robotics and Automation (ICRA)*, 2013, pp. 2041–2046.

[5] B. B. Kang, H. Lee, H. In, U. Jeong, J. Chung, and K.-J. Cho, "Development of a polymer-based tendon-driven wearable robotic hand," in *IEEE International Conference on Robotics and Automation (ICRA)*, 2016, pp. 3750–3755.

[6] V. Mathiowetz, N. Kashman, G. Volland, K. Weber, M. Dowe, S. Rogers *et al.*, "Grip and pinch strength: normative data for adults," *Arch Phys Med Rehabil*, vol. 66, no. 2, pp. 69–74, 1985.

[7] I. N. Gaiser, C. Pylatiuk, S. Schulz, A. Kargov, R. Oberle, and T. Werner, "The fluidhand iii: A multifunctional prosthetic hand," *JPO: Journal of Prosthetics and Orthotics*, vol. 21, no. 2, pp. 91–96, 2009.

[8] A. D. Astin, "Finger force capability: measurement and prediction using anthropometric and myoelectric measures," 1999.

[9] P. Polygerinos, K. C. Galloway, E. Savage, M. Herman, K. O'Donnell, and C. J. Walsh, "Soft robotic glove for hand rehabilitation and task specific training," in *IEEE International Conference on Robotics and Automation (ICRA)*, 2015, pp. 2913–2919.

[10] C.-Y. Chu and R. M. Patterson, "Soft robotic devices for hand rehabilitation and assistance: a narrative review," *Journal of NeuroEngineering and Rehabilitation*, vol. 15, no. 1, p. 9, 2018.

[11] P. Maciejasz, J. Eschweiler, K. Gerlach-Hahn, A. Jansen-Troy, and S. Leonhardt, "A survey on robotic devices for upper limb rehabilitation," *Journal of neuroengineering and rehabilitation*, vol. 11, no. 1, p. 3, 2014.

[12] M. Fontana, A. Dettori, F. Salsedo, and M. Bergamasco, "Mechanical design of a novel hand exoskeleton for accurate force displaying," in *IEEE International Conference on Robotics and Automation (ICRA)*, 2009, pp. 1704–1709.

[13] M. A. Delph, S. A. Fischer, P. W. Gauthier, C. H. M. Luna, E. A. Clancy, and G. S. Fischer, "A soft robotic exomusculature glove with integrated semg sensing for hand rehabilitation," in *IEEE International Conference on Rehabilitation Robotics (ICORR)*, 2013, pp. 1–7.

[14] M. Nilsson, J. Ingvast, J. Wikander, and H. von Holst, "The soft extra muscle system for improving the grasping capability in neurological rehabilitation," in *IEEE EMBS Conference on Biomedical Engineering and Sciences (IECBES)*, 2012, pp. 412–417.

[15] J. Rogers, B. Peters, E. Laske, and E. McBryan, "Development and testing of robotically assisted extravehicular activity gloves." 47th International Conference on Environmental Systems, 2017.

[16] P. Polygerinos, Z. Wang, K. C. Galloway, R. J. Wood, and C. J. Walsh, "Soft robotic glove for combined assistance and at-home rehabilitation," *Robotics and Autonomous Systems*, vol. 73, pp. 135–143, 2015.

[17] H. K. Yap, J. H. Lim, F. Nasrallah, and C.-H. Yeow, "Design and preliminary feasibility study of a soft robotic glove for hand function assistance in stroke survivors," *Frontiers in neuroscience*, vol. 11, p. 547, 2017.

[18] J. T. Belter and A. M. Dollar, "Novel differential mechanism enabling two dof from a single actuator: Application to a prosthetic hand," in *IEEE International Conference on Rehabilitation Robotics (ICORR)*, 2013, pp. 1–6.

[19] G. P. Kontoudis, M. V. Liarokapis, A. G. Zisimatos, C. I. Mavrogiannis, and K. J. Kyriakopoulos, "Open-source, anthropomorphic, underactuated robot hands with a selectively lockable differential mechanism: Towards affordable prostheses," in *IEEE/RSJ International Conference on Intelligent Robots and Systems (IROS)*, 2015, pp. 5857–5862.

[20] L. Gerez and M. Liarokapis, "A compact ratchet clutch mechanism for fine tendon termination and adjustment," in *IEEE/ASME International Conference on Advanced Intelligent Mechatronics (AIM)*, 2018, pp. 1390–1395.

[21] I. M. Bullock, J. Z. Zheng, S. De La Rosa, C. Guertler, and A. M. Dollar, "Grasp frequency and usage in daily household and machine shop tasks," *IEEE transactions on haptics*, vol. 6, pp. 296–308, 2013.

[22] U. Jeong, H. In, H. Lee, B. B. Kang, and K.-J. Cho, "Investigation on the control strategy of soft wearable robotic hand with slack enabling tendon actuator," in *IEEE International Conference on Robotics and Automation (ICRA)*, 2015, pp. 5004–5009.

[23] M. Xiloyannis, L. Cappello, D. B. Khanh, S.-C. Yen, and L. Masia, "Modelling and design of a synergy-based actuator for a tendon-driven soft robotic glove," in *IEEE International Conference on Biomedical Robotics and Biomechatronics (BioRob)*, 2016, pp. 1213–1219.

[24] G. Bain, N. Polites, B. Higgs, R. Heptinstall, and A. McGrath, "The functional range of motion of the finger joints," *Journal of Hand Surgery (European Volume)*, vol. 40, no. 4, pp. 406–411, 2015.

[25] M. R. Cutkosky, "On grasp choice, grasp models, and the design of hands for manufacturing tasks," *IEEE Transactions on robotics and automation*, vol. 5, no. 3, pp. 269–279, 1989.

[26] T. Iberall, "Human prehension and dexterous robot hands," *The International Journal of Robotics Research*, vol. 16, no. 3, pp. 285–299, 1997.

[27] N. Smaby, M. E. Johanson, B. Baker, D. E. Kenney, W. M. Murray, and V. R. Hentz, "Identification of key pinch forces required to complete functional tasks." *Journal of Rehabilitation Research & Development*, vol. 41, no. 2, 2004.

[28] G. Langevin, "Inmoov - open source 3d printed life-size robot." [Online]. Available: http://www.inmoov.fr/